

The UKIRT Infrared Deep Sky Survey Second Data Release

S. J. Warren¹, N. J. G. Cross², S. Dye³, N. C. Hambly², O. Almaini⁴, A. C. Edge⁵, P. C. Hewett⁶, S. T. Hodgkin⁶, M. J. Irwin⁶, R. F. Jameson⁷, A. Lawrence², P. W. Lucas⁸, D. J. Mortlock¹, A. J. Adamson⁹, J. Bryant², R. S. Collins², C. J. Davis⁹, J. P. Emerson¹⁰, D. W. Evans⁶, E. A. Gonzales-Solares⁶, P. Hirst^{9,11}, T. H. Kerr⁹, J. R. Lewis⁶, R. G. Mann², M. G. Rawlings⁹, M. A. Read², M. Riello⁶, E. T. W. Sutorius², W. P. Varricatt⁹

ABSTRACT

The UKIRT Infrared Deep Sky Survey (UKIDSS) is a set of five large near-infrared surveys, covering a complementary range of areas, depths, and Galactic latitudes. The UKIDSS Second Data Release (DR2) includes the First Data Release (DR1), with minor improvements, plus new data for the LAS, GPS, GCS, and DXS, from observations made over 2006 May through July (when the UDS was unobservable). DR2 is being staged in two parts. The first part excludes the GPS, and took place on 2007 March 1. The GPS will form the second part, which is anticipated for 2007 March 31, and this paper will be updated at that time with the GPS details. The first part of DR2 includes 340 deg² of multicolour data to (Vega) $K = 18$, complete in the $YJHK$ set for the LAS, and the $ZYJHK$ set for the GCS. DR2 includes nearly 7 deg² of deep JK data (DXS, UDS) to an average depth $K = 21$. In addition the release includes a comparable quantity of data where coverage of the filter set for any survey is incomplete. We document changes that have occurred since DR1 to the pipeline, calibration, and archive procedures. The two most noteworthy changes are presentation of the data in a single database (compared to two previously), and provision of additional error flags for detected sources, flagging potentially spurious artifacts, corrupted data and suspected cross-talk sources. We summarise the contents of each of the surveys in terms of filters, areas, and depths.

Subject headings: astronomical data bases: surveys – infrared: general

¹Astrophysics Group, Imperial College London, Blackett Laboratory, Prince Consort Road, London, SW7 2AZ, U.K.

²Scottish Universities Physics Alliance (SUPA), Institute for Astronomy, School of Physics, University of Edinburgh, Royal Observatory, Blackford Hill, Edinburgh, EH9 3HJ, U.K.

³Cardiff University, School of Physics & Astronomy, Queens Buildings, The Parade, Cardiff, CF24 3AA, U.K.

⁴School of Physics and Astronomy, University of Nottingham, University Park, Nottingham, NG7 2RD, U.K.

⁵Department of Physics, Durham University, South Road, DH1 3LE, U.K.

⁶Institute of Astronomy, Madingley Rd., Cambridge, CB3 0HA, U.K.

⁷Department of Physics and Astronomy, University of Leicester, Leicester, LE1 7RH, U.K.

⁸Centre for Astrophysics Research, Science and Technology Research Institute, University of Hertfordshire, Hat-

1. Introduction

UKIDSS is the UKIRT Infrared Deep Sky Survey (Lawrence et al. 2007), carried out using the Wide Field Camera (WFCAM; Casali et al. 2007) installed on the United Kingdom Infrared Telescope (UKIRT). Data acquisition for the survey started in 2005 May. The Early Data Release (EDR; Dye et al. 2006, hereafter D06),

field, AL10 9AB, U.K.

⁹Joint Astronomy Centre, 660 N. A'ohoku Place, University Park, Hilo, Hawaii 96720, U.S.A.

¹⁰Astronomy Unit, School of Mathematical Sciences, Queen Mary, University of London, Mile End Road, London E1 4NS, U.K.

¹¹Gemini Observatory, Northern Operations Center, 670 North A'ohoku Place, Hilo, HI96720, U.S.A.

a prototype dataset, and the First Data Release (DR1; Warren et al. 2007, hereafter W07), the first release of survey-quality data, took place in 2006. This paper describes the Second Data Release (DR2). The data are available from the WFCAM science archive (WSA) at <http://surveys.roe.ac.uk/wsa>.

UKIDSS is a programme of five imaging surveys that each uses some or all of the broadband filter complement *ZYJHK*, and that span a range of areas, depths, and Galactic latitudes. There are three high Galactic latitude surveys, providing complementary combinations of area and depth; the Large Area Survey (LAS), will cover 4000 deg^2 to $K = 18$, the Deep ExtraGalactic Survey (DXS), 35 deg^2 to $K = 21$, and the Ultra Deep Survey (UDS), 0.8 deg^2 to $K = 23$. There are two other wide surveys to $K = 18$, aimed at targets in the Milky Way; the Galactic Plane Survey (GPS) will cover 1900 deg^2 , and the Galactic Clusters Survey (GCS) 1100 deg^2 . The complete UKIDSS programme is scheduled to take seven years, requiring ~ 1000 nights on UKIRT. The current implementation strategy is focused on completing an intermediate set of goals, defined by the ‘2-year plan’ detailed in D06. All magnitudes quoted in this paper use the Vega system described by Hewett et al. (2006). Depths, where not explicitly specified, are the total brightness of a point source for which the flux integrated in a $2''$ diameter aperture is detected at 5σ .

A set of five baseline papers provides the relevant technical background information for the surveys. The overview of the programme is given by Lawrence et al. (2007). This sets out the science goals that drove the design of the survey programme, and details the final coverage that will be achieved, in terms of fields, areas, depths, and filters. The camera is described in detail by Casali et al. (2007), and the *ZYJHK* photometric system is characterised by Hewett et al. (2006), who provide synthetic colours for a wide range of types of star, galaxy, and quasar. Details of the data pipeline and data archive will appear in Irwin et al. (2007, in prep.) and Hambly et al. (2007, in prep.), respectively.

Each UKIDSS data release includes the data contained in previous releases, together with new data. The instrument is scheduled in blocks of time of typically three to six months duration.

Current policy is that each observing block results in a data release. DR1 comprised data from the 2005A and 2005B observing blocks. DR2 includes the relatively short 2006A observing block, which ran over 2006 May to July. DR3 will be much larger, including the consecutive 2006B and 2007A blocks, running over 2006 November to 2007 May.

Each UKIDSS data release is accompanied by a paper summarising the contents of the release, and detailing procedural changes since the previous release. The EDR provided a small prototype dataset, and represented a step towards regular release of survey-quality data. The EDR paper, D06, is a self-contained summary of all information relevant to understanding the contents of the EDR. It also serves as the baseline paper for technical details for all releases. Besides a summary of the contents of the EDR database, D06 includes relevant details of the camera design, the observational implementation (integration times, microstepping), the pipeline and calibration, data artifacts, and the quality control procedures, as well as a brief guide to querying the archive. Subsequent papers summarise the contents of the particular release, together with a description of changes to the implementation, pipeline, calibration, quality control, and archive procedures. The DR1 paper, W07, also included plots summarising the distributions of seeing, sky brightness, and airmass over the dataset.

The present paper covers DR2. DR2 includes new data for the LAS, GPS, GCS, and DXS, but not the UDS which was unobservable in 2006A. The UDS therefore appears in DR2 in identical form to DR1. Details concerning the UDS may be found in W07, and no further mention is made here. DR2 is appearing in two stages. The first stage, released on 2007 March 1, is complete except for the GPS. The GPS data will be released in stage two, scheduled for 2007 March 31. In Section 2 we detail changes between DR1 and DR2 to the pipeline, calibration, and archive procedures. In Section 3 we summarise the contents of DR2.

2. Update

D06 contains details of the implementation, pipeline, calibration, quality control, and archive procedures applied to the EDR data, and a glossary of technical terms. W07 details changes

to these procedures between the EDR and DR1. In this section we detail further changes since DR1. These include mostly minor changes to the pipeline, calibration, and archive procedures. The implementation and quality control procedures are virtually unchanged. During 2006A, fields were not observed when the moon was within 30deg, in order to avoid moon ghosts (D06, W07). A baffle was installed after the end of 2006A that appears to have eliminated moon ghosts altogether, and the restriction has been removed for 2006B.

2.1. Pipeline and calibration

2.1.1. Pipeline

For DR2 all 2005A WFCAM data were reprocessed from scratch from the raw data. The 2005A data were first released in the EDR, and were not revised for DR1. The main changes in the image processing aspects between EDR and DR1, and used in processing the 2005B data, were an improved sky correction strategy more closely linked to the observing block structure (MSBs), and the application of the cross-talk suppression algorithm (W07). Further minor improvements have been made to the sky correction strategy since DR1. Therefore the 2005A and 2006A data benefit from these improvements. The 2005B data have not been reprocessed since DR1 however.

Further small changes to the cataloguing software, mainly related to improving the object detection filter, have also been made since DR1 and were used in the catalogue (re)generation for the 2005A data. All of the new 2006A WFCAM data were processed with the latest versions of the pipeline software.

Several minor improvements to the photometric calibration procedure have also been implemented since DR1 in an attempt to reduce any dependence of the derived photometric zero-points on Galactic coordinates, due to, for example, varying dwarf-giant ratios, extinction and extreme colour objects.

As previously, each frame is calibrated using 2MASS stars in the frame, converting the 2MASS photometry to the WFCAM system using appropriate colour equations. The zero point for each detector is now provided as the attribute `photZPCat` in the table `MultiframeDetector`. The attribute `photZP` in the table `Multiframe`

has been deprecated. The updated WFCAM calibration uses a restricted (extinction-corrected) colour range of $0 < J_2 - K_2 < 1$ (the subscript 2 standing for 2MASS) to help exclude late-type giants, unusual objects and heavily reddened stars. Also, as a result of discovering a correlation of the derived *Y*- and *Z*-band zero points with Galactic extinction, particularly in regions of heavy extinction, an extra extinction-dependent calibration term has been included. The revised colour equations are as follows:

$$\begin{aligned} Z &= J_2 + 0.95(J_2 - H_2) + 0.39E(B - V)' \\ Y &= J_2 + 0.50(J_2 - H_2) + 0.16E(B - V)' \\ J &= J_2 - 0.065(J_2 - H_2) + 0.015E(B - V)' \\ H &= H_2 + 0.07(J_2 - H_2) + 0.005E(B - V)' - 0.03 \\ K &= K_2 + 0.01(J_2 - K_2) + 0.005E(B - V)' \end{aligned}$$

Here $E(B - V)'$ is the reddening computed using the prescription of Bonifacio et al. (2000), from the data of Schlegel et al. (1998). The corrections for reddening are small in the *JHK* bands and in practice also for the *Y* band which is only used in the LAS where the extinction is low. The reddening corrections for the *Z* band, only used in the GCS, are large in fields with large reddening, and should be treated with caution.

The revised colour equations produce a more stable calibration for the *Y* and *Z* bands (but generally have little impact on the *JHK* calibration). In addition, errors on the individual 2MASS-derived zero-points are now included together with measures summarising the photometric quality of the night and the overall nightly average zero-point.

W07 note that there is evidence for an overall zero-point offset with respect to the Vega system for the *Y* and *Z* bands. An analysis of this issue is deferred to DR3.

2.2. Archive

In previous releases two databases were provided, one containing all the data (called EDR+, DR1+), and a second, a subset of the larger database, containing data for all fields observed with the full filter complement for the particular survey (called EDR, DR1). For DR2 there is only one database, DR2+. Nevertheless *views* are provided of the source tables for each survey, e.g. *lasYJHKsource* in order to provide the equivalent functionality.

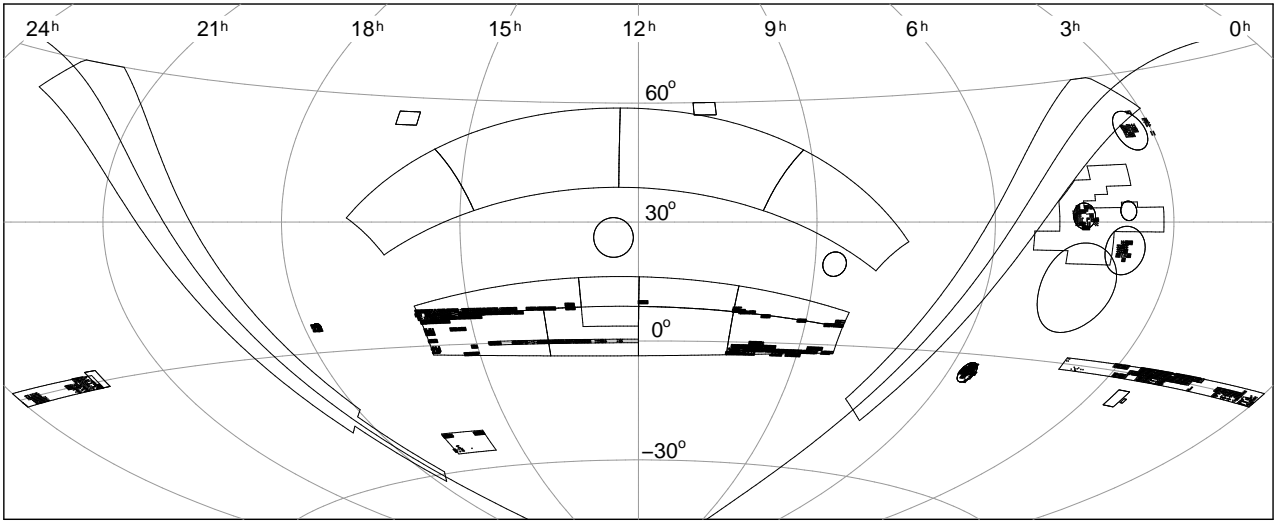


Fig. 1.— Plot showing regions with full filter coverage for the LAS (*YJHK*) and GCS (*ZYJHK*). The outlines are the boundaries of the surveys (see Lawrence et al. (2007), and D06 for details), and the filled regions are the fields included in DR2. The three LAS zones are the thin equatorial stripe, and the two broad bands in the centre. All other regions containing data are GCS fields.

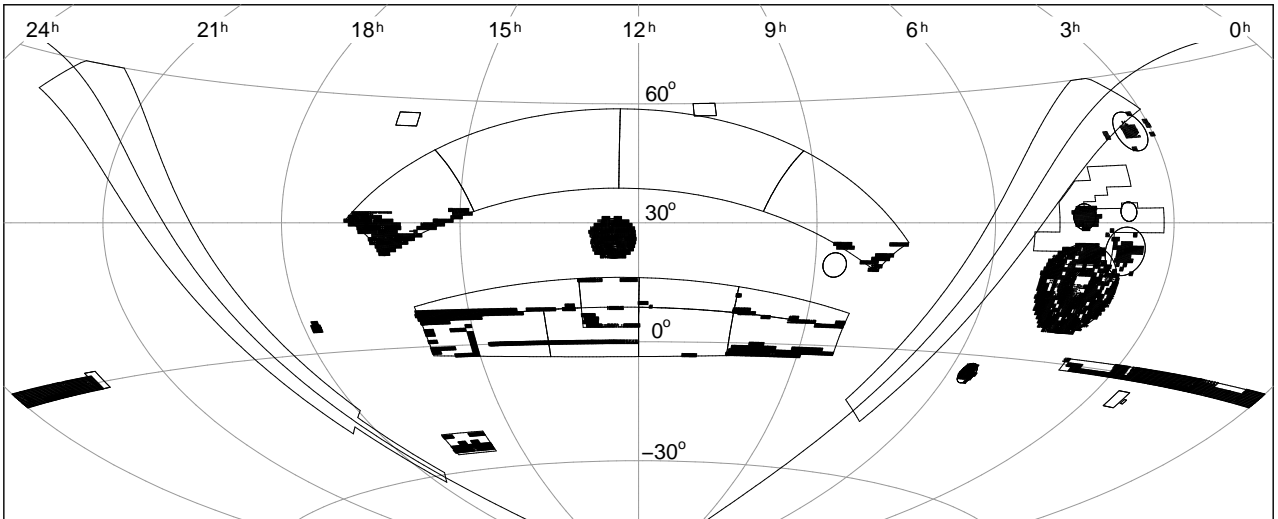


Fig. 2.— Plot showing regions of the LAS and GCS with coverage with any filters. The outlines are the boundaries of the surveys (see Lawrence et al. (2007), and D06 for details), and the filled regions are the fields included in DR2. The three LAS regions are the thin equatorial stripe, and the two broad bands in the centre. Observations in the northern LAS block are first-epoch *J*-band only. All other regions containing data are GCS fields.

A significant improvement over DR1 is the provision of quality error bit flags for each detected source. In the detection tables the attribute is `ppErrBits`, and in the source tables the appropriate filter name is appended, e.g. `yppErrBits`, `j_1ppErrBits`. The attribute is a 32-bit integer where each bit can be set to 1 to flag up to 32 different quality issues. The quality issues are ranked in severity, with the more severe issues assigned to higher bits. Currently only five bits are set as follows: Bit 4 = the source is the offspring of deblending, Bit 6 = a bad pixel exists in the default aperture (1" radius), Bit 16 = the source is likely to contain saturated pixels, Bit 19 = the source is likely to be either cross-talk or a real source affected by cross-talk (see D06 and W07 for details on cross-talk), Bit 22 = the source is likely to include incomplete data as a consequence of lying close to the frame boundary. Therefore by converting `ppErrBits` to binary it is possible to filter out sources with particular quality issues. Alternatively a threshold can be set e.g. `ppErrBits < 32` to select sources with only very minor quality issues.¹

In addition the seaming algorithm has been improved since DR1. The seaming algorithm deals with sources that are detected in separate (two or more) multiframes that overlap. To decide which detection will be designated primary a sequence of discriminants is considered, until a preference is established: first the number of filters in which the source is detected, second the count from `ppErrBits`, and finally the distance of the source from the detector edge.

UKIDSS DR2 is crossmatched with SDSS DR5 (Adelman-McCarthy et al. 2007), updated from SDSS DR3 for UKIDSS DR1. Note also that new crossmatching with catalogues from the Millennium Galaxy Catalogue (Liske et al. 2003) and the NRAO VLA Sky Survey (Condon et al. 1998) is provided for DR2.

3. Summary of the contents of DR2

3.1. LAS, GCS

For the shallow surveys, LAS, GCS, Figs 1 and 2 plot the survey coverage in DR2. Fig. 1 illus-

trates the sky coverage of fields where the filter set for the particular survey is complete, while Fig. 2 shows all fields in which any data have been taken. The new LAS data are confined to the region $10^{\text{h}}53^{\text{m}} < RA < 16^{\text{h}}50^{\text{m}}$. The new observations in the northern block, near $RA = 16^{\text{h}}$, are J-band only, and are first epoch observations for proper motions in fields that will later be reobserved in the full filter complement, after a minimum interval of two years (D06).

Details of the summed area covered, by filter, in each of the shallow surveys, LAS, and GCS, are provided in Table 1. For each survey, the table provides the area covered in a particular filter, the area covered by all filters, and the area covered by any filter. Table 2 provides the median 5σ depth (as defined in D06) achieved in each band in each of the two surveys. These values are slightly deeper than those for DR1, provided in W07.

A quirk persists from DR1 (see section 4.1 in W07) which results in a small number of LAS sources recorded in the archive as detected in *YJ* only, coincident with distinct sources (in reality the same sources) recorded as detected in *HK* only.

¹Further details are provided at <http://surveys.roe.ac.uk/wsa/drtwo/ppErrBits.html>

TABLE 1
 COVERAGE OF THE SHALLOW SURVEYS (DEG²) IN DR2 (GPS DETAILS WILL BE ADDED WHEN AVAILABLE).

Survey	all	filter					
	filters	<i>Z</i>	<i>Y</i>	<i>J</i>	<i>H</i>	<i>K</i>	any
LAS	282	-	341	505	477	476	685
GCS	57	80	81	83	116	478	496
total	339	80	433	588	593	954	1181

TABLE 2
 THE MEDIAN 5σ POINT SOURCE DEPTH BY FILTER IN THE DR2 DATABASE FOR THE SHALLOW SURVEYS (GPS DETAILS WILL BE ADDED WHEN AVAILABLE).

Filter	LAS	GCS
<i>Z</i>	-	20.54
<i>Y</i>	20.23	20.16
<i>J</i>	19.61	19.59
<i>H</i>	18.90	18.87
<i>K</i>	18.23	18.20

TABLE 3

THE DXS *depleavstack* MULTIFRAMES. THE FIELD, SUB-FIELD CODE, AND BASE COORDINATES ARE LISTED, THEN, FOR J AND K SUCCESSIVELY, THE TOTAL INTEGRATION TIME, 5σ DEPTH, SEEING, AND ELLIPTICITY $e = 1 - b/a$.

Field	Sub field	RA	Dec	t_{tot}	Depth	seeing	ellip.	t_{tot}	Depth	seeing	ellip.
				J				K			
XMM-LSS	1.00	36.5752020	-4.7496444	6400	22.195	0.88	0.05	7040	20.845	0.76	0.08
XMM-LSS	1.10	36.5803542	-4.5294528	7680	22.265	0.86	0.06	8320	20.935	0.74	0.09
XMM-LSS	1.01	36.8012000	-4.7496444	7680	22.245	0.86	0.05	7680	20.885	0.77	0.08
XMM-LSS	1.11	36.8012000	-4.5294528	7040	22.275	0.86	0.05	5760	20.735	0.75	0.09
XMM-LSS	2.00	35.7098417	-4.7496444	-	-	-	-	6400	20.675	0.93	0.08
XMM-LSS	2.10	35.7098417	-4.5294528	-	-	-	-	7040	20.715	0.91	0.07
XMM-LSS	2.01	35.9306875	-4.7496444	-	-	-	-	7040	20.695	0.91	0.08
XMM-LSS	2.11	35.9306875	-4.5294528	-	-	-	-	6400	20.675	0.89	0.07
XMM-LSS	3.00	35.7094541	-3.8688833	-	-	-	-	640	19.325	1.17	0.11
XMM-LSS	3.01	35.9300625	-3.8688833	-	-	-	-	640	19.375	1.12	0.10
Lockman Hole	1.00	163.3623000	57.4753556	1280	21.565	1.06	0.10	12600	20.995	0.93	0.09
Lockman Hole	1.10	163.3623000	57.6955472	1280	21.575	1.06	0.08	13960	21.055	0.98	0.09
Lockman Hole	1.01	163.7756170	57.4753556	640	21.085	1.16	0.06	13820	21.025	0.99	0.08
Lockman Hole	1.11	163.7756170	57.6955472	1280	21.465	1.15	0.08	11820	20.965	0.98	0.08
Lockman Hole	6.00	161.6707620	59.1223000	-	-	-	-	8840	20.765	1.06	0.08
Lockman Hole	6.10	161.6707620	59.3424917	-	-	-	-	9840	20.855	1.05	0.08
Lockman Hole	6.01	162.1040380	59.1223000	-	-	-	-	9340	20.815	1.05	0.06
Lockman Hole	6.11	162.1040380	59.3424917	-	-	-	-	8700	20.745	1.06	0.08
ELAIS N1	1.00	242.5994000	54.5031333	6560	21.785	1.01	0.06	8000	20.675	0.99	0.08
ELAIS N1	1.10	242.5994000	54.7233250	6060	21.785	0.96	0.07	8500	20.795	0.98	0.08
ELAIS N1	1.01	242.9817370	54.5031333	8480	21.855	0.99	0.07	9000	20.845	0.98	0.09
ELAIS N1	1.11	242.9817370	54.7233250	9480	21.845	1.04	0.07	8000	20.725	0.97	0.09
ELAIS N1	2.00	241.1580080	54.5031333	8320	22.125	0.92	0.05	9400	20.815	0.89	0.08
ELAIS N1	2.10	241.1580080	54.7233250	7680	22.075	0.93	0.05	7620	20.595	0.91	0.09
ELAIS N1	2.01	241.5403460	54.5031333	8960	22.115	0.94	0.05	9260	20.785	0.89	0.08
ELAIS N1	2.11	241.5403460	54.7233250	6400	21.955	0.94	0.05	8400	20.715	0.87	0.08
ELAIS N1	3.00	241.1364170	55.3170222	-	-	-	-	500	19.165	1.08	0.05
ELAIS N1	3.10	241.1364170	55.5372139	-	-	-	-	500	19.215	1.09	0.05
ELAIS N1	3.01	241.5266580	55.3170222	-	-	-	-	500	19.275	0.96	0.09
ELAIS N1	3.11	241.5266580	55.5372139	-	-	-	-	500	19.215	0.95	0.12
ELAIS N1	4.00	242.6111380	55.3170222	-	-	-	-	500	19.405	0.83	0.09
ELAIS N1	4.10	242.6111380	55.5372139	-	-	-	-	500	19.415	0.81	0.11
ELAIS N1	4.01	243.0013830	55.3170222	-	-	-	-	500	19.405	0.86	0.09

3.2. DXS

The DXS is targeting the following four fields: XMM-LSS ($2^{\text{h}}25^{\text{m}}, -4^{\circ}30'$), the Lockman Hole ($10^{\text{h}}57^{\text{m}}, +57^{\circ}40'$), Elais N1 ($16^{\text{h}}10^{\text{m}}, +54^{\circ}00'$), and VIMOS 4 ($22^{\text{h}}17^{\text{m}}, +0^{\circ}20'$). The fields are plotted as small quadrilaterals in Figs 1 and 2. Eventually each field will be tessellated by 12 tiles, each of four pointings. The observing strategy (Lawrence et al. 2007) aims to reach full depth in a tile, $K = 21$, $J = 22.5$, before moving to the next tile. Depth is built up by a series of observations of length 640s (500s in 2005A), known as intermediate stacks. All the intermediate stacks for any pointing are combined to create *depleavstack* multiframes (D06). All intermediate stack and *depleavstack* multiframes are included in a release.

In DR2 the numbers of *depleavstack* multiframes are 55 in K and 32 in J . Details of all the DXS *depleavstacks* are provided in Table 3. The first column provides the field name, and the second is a code identifying the sub-field, in the form *Tile.XY*, where XY are binary coordinates

specifying one of four multiframe positions that make up a tile. Columns three and four provide the coordinates of the base position, which is the centre of the field of view (which is a point not imaged by the detectors). The remaining columns give the total integration time t_{tot} of the frames contributing to the stack (i.e. excluding deprecated frames), the 5σ depth, the seeing, and the ellipticity, for the J and K frames.

In total the DXS contains fields with deep JK coverage, reaching $K \sim 21$, over 6 deg^2 .

REFERENCES

- Adelman-McCarthy, J. K., et al. 2007, ApJS, submitted
- Bonifacio, P., Monai, S., & Beers, T. C. 2000, AJ, 120, 2065
- Casali, M., et al., 2007, A&A, in press
- Condon, J. J., Cotton, W. D., Greisen, E. W., Yin, Q. F., Perley, R. A., Taylor, G. B., & Broderick, J. J., 1998, AJ, 115, 1693
- Dye, S., Warren, S. J., Hambly, N. C., et al., 2006, MNRAS, 372, 1227
- Hewett, P. C., Warren, S. J., Leggett, S. K., & Hodgkin, S. T. 2006, MNRAS, 367, 454
- Lawrence, A., et al., 2007, MNRAS, submitted (astro-ph/0604426)
- Liske, J., Lemon, D. J., Driver, S. P., Cross, N. J. G., Couch, W. J., 2003, MNRAS, 344, 307
- Schlegel, D. J., Finkbeiner, D. P., & Davis, M. 1998, ApJ, 500, 525
- Warren S. J., et al., 2007, MNRAS, 375, 213

TABLE 3—*Continued*

Field	Sub field	RA J2000	Dec	t_{tot} s	Depth mag. <i>J</i>	seeing " <i>J</i>	ellip.	t_{tot} s	Depth mag. <i>K</i>	seeing " <i>K</i>	ellip.
VIMOS 4	1.00	334.2667460	0.1698000	8820	22.175	0.89	0.04	10400	20.945	0.83	0.06
VIMOS 4	1.10	334.2667460	0.3899917	10740	22.285	0.86	0.04	12820	21.085	0.79	0.06
VIMOS 4	1.01	334.4869460	0.1698000	10100	22.355	0.84	0.04	10900	21.055	0.80	0.06
VIMOS 4	1.11	334.4869460	0.3899917	6900	22.165	0.88	0.05	10260	20.975	0.85	0.06
VIMOS 4	2.00	335.1420250	0.1817444	5120	21.855	0.92	0.04	8960	20.945	0.75	0.06
VIMOS 4	2.10	335.1420250	0.4019361	4480	21.845	0.93	0.03	10240	20.965	0.74	0.06
VIMOS 4	2.01	335.3622250	0.1817444	5120	21.845	1.02	0.04	10240	20.945	0.74	0.06
VIMOS 4	2.11	335.3622250	0.4019361	5760	21.925	0.94	0.04	9600	20.885	0.75	0.06
VIMOS 4	3.00	335.1420790	1.0559111	11520	22.325	0.85	0.04	10240	20.795	0.94	0.06
VIMOS 4	3.10	335.1420790	1.2761028	11520	22.375	0.87	0.04	11520	20.905	0.98	0.05
VIMOS 4	3.01	335.3623330	1.0559111	9600	22.315	0.88	0.04	11520	20.885	0.98	0.05
VIMOS 4	3.11	335.3623330	1.2761028	11520	22.365	0.88	0.05	10880	20.895	0.93	0.06
VIMOS 4	4.00	334.2668040	1.0559111	1920	21.535	0.98	0.04	10240	20.915	0.85	0.06
VIMOS 4	4.10	334.2668040	1.2761028	2560	21.725	0.93	0.03	12160	20.975	0.87	0.05
VIMOS 4	4.01	334.4870580	1.0559111	1920	21.515	1.00	0.04	14720	21.085	0.86	0.06
VIMOS 4	4.11	334.4870580	1.2761028	1280	21.285	0.93	0.04	12800	21.035	0.87	0.06
VIMOS 4	5.00	333.3940250	1.0559111	-	-	-	-	640	19.345	1.03	0.12
VIMOS 4	5.10	333.3940250	1.2761028	-	-	-	-	640	19.235	1.15	0.13
VIMOS 4	6.00	333.3939708	0.2064666	-	-	-	-	640	19.285	1.15	0.10
VIMOS 4	6.10	333.3939708	0.4266583	-	-	-	-	640	19.385	1.06	0.05
VIMOS 4	6.01	333.6141708	0.2064666	-	-	-	-	640	19.215	1.10	0.03
VIMOS 4	6.11	333.6141708	0.4266583	-	-	-	-	640	19.365	1.05	0.03